

Applicability of Fly Neighborly Noise Recommendations to UAM Quadrotors Undergoing Steady Maneuvers

Sesi Kottapalli *

Aeromechanics Office
NASA Ames Research Center
Moffett Field, CA, USA

Christopher Silva

D. Douglas Boyd, Jr.
Aeroacoustics Branch
NASA Langley Research Center
Hampton, VA, USA

ABSTRACT

This initial study examines whether the Helicopter Association International (HAI) Fly Neighborly operational recommendations that are based on single main rotor/tail rotor configurations will hold for non-conventional UAM rotorcraft with multiple rotors. The 6-occupant quadrotor concept vehicle designed under the NASA Revolutionary Vertical Lift Technology (RVLT) Project is studied. The tip speed is 550 ft/sec, with three blades per rotor (“550/3”). Predictions are made for three steady maneuvers: level turns, descending turns, and climbing turns. The RVLT Toolchain is exercised using CAMRAD II, pyaaron/AARON/ANOPP2 and a beta version of AMAT (ANOPP2 Mission Analysis Tool). AMAT provides functionality to acoustically model the curved flight paths associated with maneuvers. In addition to quadrotor trim and performance, this study includes analysis of azimuthal variations of the vertical blade loading and its derivative in the form of contour plots on a rotor plane and line plots at one radial location ($r/R=0.765$). Quadrotor noise trends are analyzed using maximum Overall Sound Pressure Level (OASPL) and Effective Perceived Noise Level (EPNL). The Fly Neighborly guideline that addresses descents (“*Level turns are quieter than descending turns*”) is predicted to hold for the RVLT Quadrotor as well.

NOTATION

550/3	quadrotor concept vehicle with tip speed=550 ft/sec and 3 blades per rotor
AARON	ANOPP2 Aeroacoustic Rotor Noise tool
AMAT	ANOPP2 Mission Analysis Tool
ANOPP2	Aircraft Noise Prediction Program - Second Generation
BB	broadband noise (trailing-edge self-noise)
BVI	blade vortex interaction
CAMRAD II	Comprehensive Analytical Model of Rotorcraft Aerodynamics and Dynamics II
climb	straight climbing flight
descent	straight descending flight,
EPNL	Effective Perceived Noise Level, EPNdB
EPNLavg	average EPNL for all three microphones, EPNdB
left-climb	left turn in climbing flight
left-descent	left turn in descending flight
left-level	left turn in level flight
level	straight level flight
loadz	blade Z-direction (vertical) load in airframe axes, + down, N/m. (-loadz) + up
loadz derivative	derivative of loadz, N/m-deg
NDARC	NASA Design and Analysis of Rotorcraft
OASPL	Overall Sound Pressure Level, dBA
OASPLmax	maximum OASPL, dBA
pyaaron	python tool to aid running AARON
RCOTools	RotorCraft Optimization Tools

right-climb	right turn in climbing flight
right-descent	right turn in descending flight
right-level	right turn in level flight
T+L	thickness plus loading noise
UAM	Urban Air Mobility

INTRODUCTION

Recently, Ref. 1 considered the practical conceptual design of quieter urban VTOL aircraft. Several concept vehicles were studied in Ref. 1, including a 6-occupant Urban Air Mobility (UAM) quadrotor, Fig. 1. For this quadrotor, Ref. 2 used the NASA Revolutionary Vertical Lift Technology (RVLT) Toolchain (Ref. 3), referred to hereafter as the “toolchain”, to identify and analyze the noise sources, with the goal of providing guidance toward best practices for an application of the toolchain. As a follow-on study to Ref. 2, which had mainly considered rigid blades, Ref. 4 studied the effect of rotor blade elasticity on UAM quadrotor acoustics.

This paper addresses the acoustics of UAM quadrotors undergoing steady maneuvers. The concept vehicle has a constant rotor tip speed of 550 ft/sec (with a corresponding RPM of 577), with three blades per rotor (550/3). The blade radius is 9 ft and the flight speed is 122 knots. Noise comparison is done using the A-weighted OASPL and EPNL metrics. Results include quadrotor trim and power quantities, vertical blade loading and its derivative, and quadrotor noise predictions.

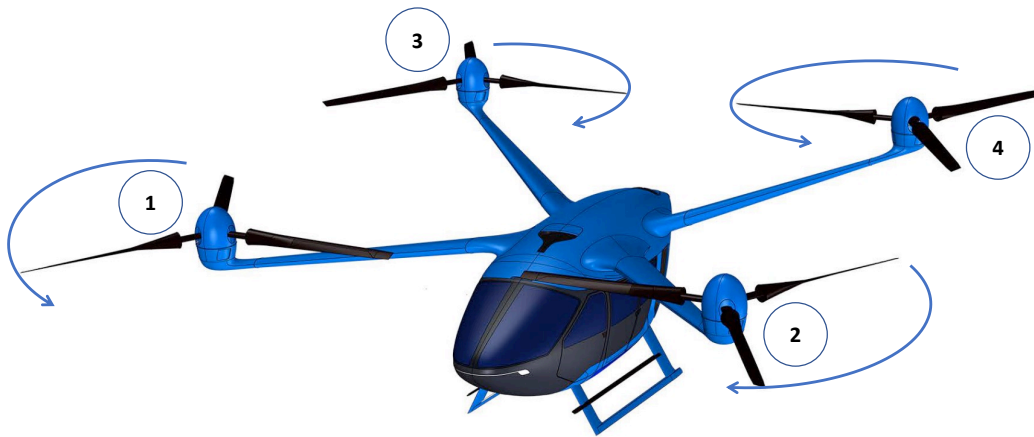
As background, Refs. 5-9 have addressed the acoustics of conventional, single main rotor helicopters undergoing maneuvers. Reference 5 concludes that “A substantial increase in the rotor noise for turning flight was found when compared to level flight at the same speed. This is due to the

* Corresponding author. Presented at the VFS 6th Decennial Aeromechanics Specialists’ Conference, Santa Clara, CA, USA Feb.6-8, 2024. This is a work of the U.S. Government and is not subject to copyright protection in the U.S.

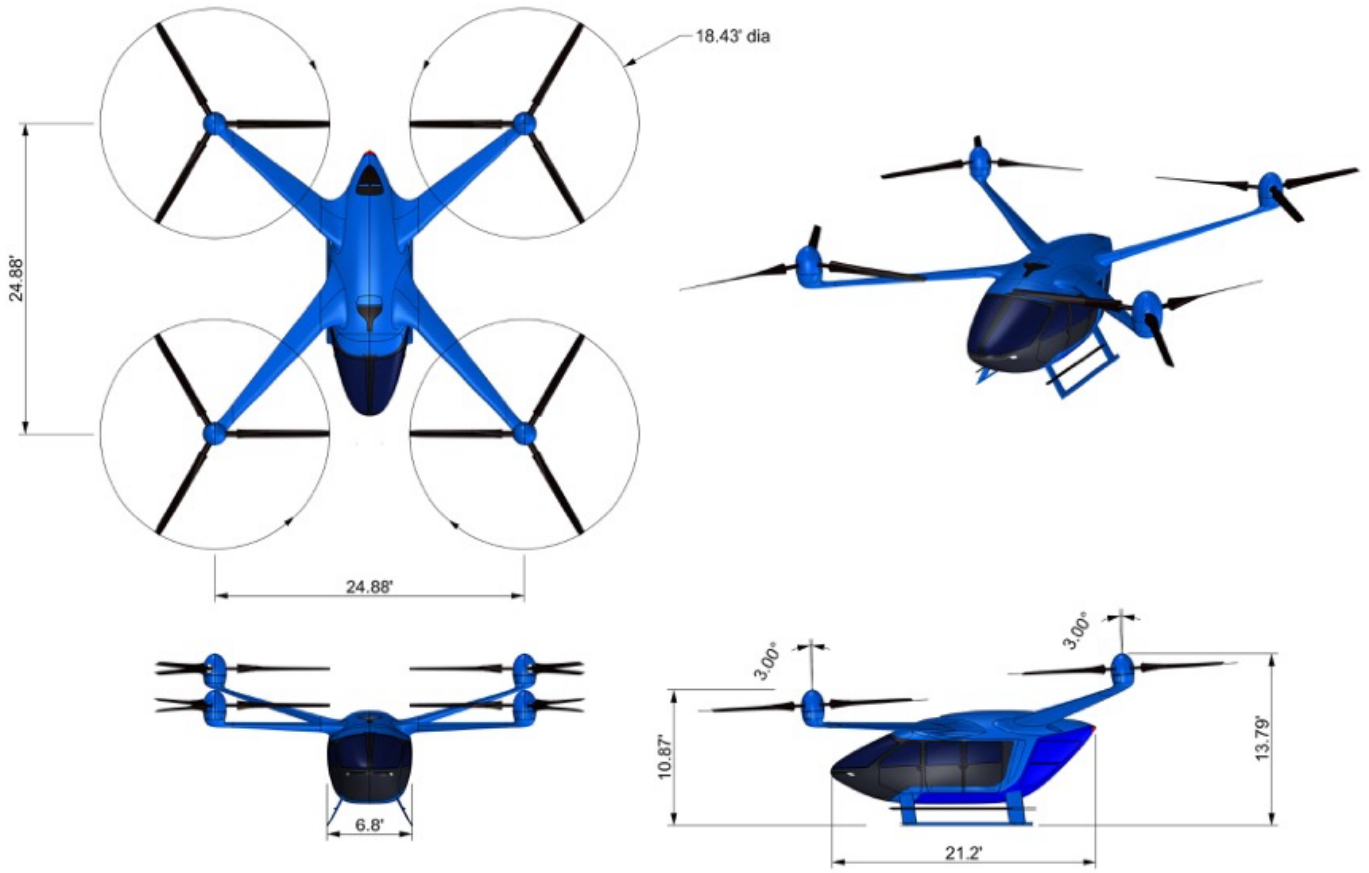
increased loading a rotor must produce in a turn.”. Reference 6 presents “the acoustic directivity for a helicopter (both main and tail rotor) in a transient descent condition and compare it to a steady three-degree descent... As a general rule, maneuver tends to increase the intensity of noise and significantly affects its directivity.”. Also, “The comparison of the two different tail rotors and the main rotor alone demonstrates the importance of including all the rotor noise sources in the acoustic prediction... the various rotors also interact with each other through the balance of forces in the vehicle flight dynamics.” (Ref. 6). Reference 7 shows that “that Bell 206B Blade Vortex Interaction (BVI) external noise gradually increases in level flight at moderate bank angles and with increasing rates of descent.” Based on extensive flight test data, Ref. 8 provides “...validated actionable guidance principles that can be given to pilots to immediately reduce their acoustic footprint during operations. This generic guidance works by keeping the rotor well away from the wake throughout the maneuver, thus increasing miss distance and reducing the occurrence of objectionable BVI noise.” For

conventional helicopters, Ref. 8 concludes, for example, that noise from level flight turns is not affected by turn direction and level flight turns are quieter than descending turns. Closely related to the conclusions of Ref. 8 are the Fly Neighborly guidelines that are based on the single main rotor helicopter configuration; these operational recommendations have been published by the Helicopter Association International (HAI), Ref. 9.

The current study analyzes the acoustics of the NASA 6-occupant quadrotor concept vehicle. This study examines whether the HAI Fly Neighborly operational recommendations are predicted to hold for this non-conventional rotorcraft with multiple rotors, Figs. 1a-1b. The RVL Toolchain and quadrotor modeling are briefly described, followed by the simulation results. The maneuvers considered in this initial study are level turns, descending turns, and climbing turns. Figure 2 shows the flight paths for these turns.



1a). Six-occupant quadrotor isometric view, marked with rotor rotation direction and numbering.



1b). Quadrotor technical drawings, Ref. 1.

Figure 1. Quadrotor geometry.

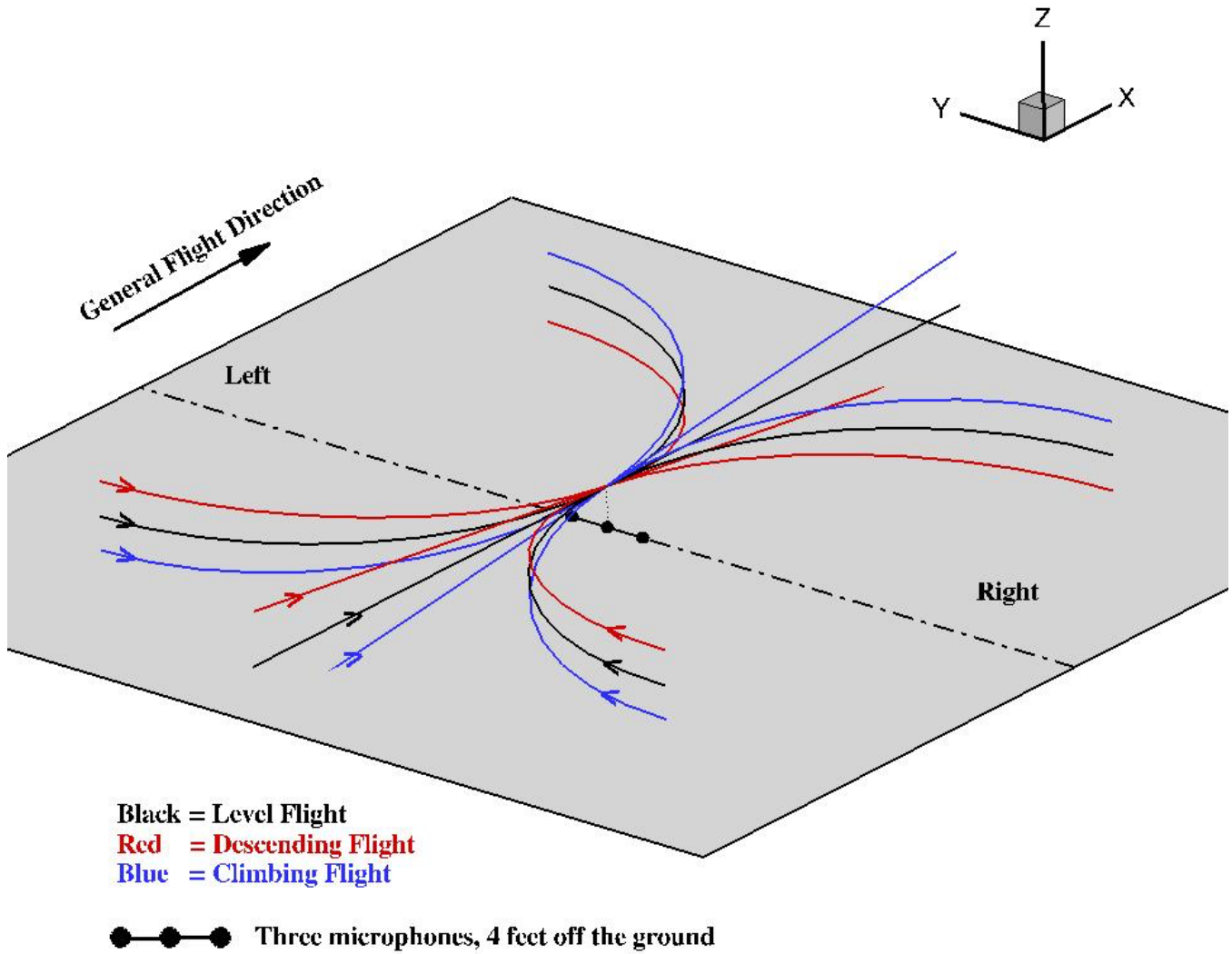


Figure 2. Semi-circular flight paths used in acoustic modeling of level, descending, and climbing turns. Curved lines depict flight paths in both directions for descending, level, and climbing flights. Each path starts closest to the reader and ends away from the reader.

RVLT TOOLCHAIN

The currently relevant part of the toolchain is discussed in Refs. 2 and 4 and only a summary is provided here. The rotorcraft comprehensive analysis CAMRAD II (Comprehensive Analytical Model of Rotorcraft Aerodynamics and Dynamics, Ref. 10) is used. RCOTools, a set of python libraries that serve as application interfaces/wrappers for the execution of CAMRAD II is also a part of the toolchain (Ref. 11). “pyaaron,” a python-based wrapper script, provides an interface for application-specific user inputs. pyaaron also extracts relevant CAMRAD II data that is then passed on to the acoustic tools.

The acoustic calculations are performed using the following tools:

- AARON (the ANOPP2 Aeroacoustic Rotor Noise tool), Ref. 12. In this context, AARON is an ANOPP2 software tool written in FORTRAN that runs the ANOPP2 Farassat Formulation 1A Function Model (AF1AIFM) for tone noise and/or the ANOPP2 Self Noise Internal Function Module (ASNIFM) for rotor broadband self noise. AARON calculates the 1/3-octave spectrum at each point of a 19x19 hemisphere underneath the vehicle. This calculation is based on the CAMRAD II outputs and a small amount of supplemental information and includes both tone sources (thickness and loading noise) and broadband noise (trailing-edge self-noise), Ref. 1.
- AMAT (ANOPP2 Mission Analysis Tool), Ref. 13. AMAT has been used to predict Noise-Power-Distance data for UAM vehicles (Ref. 14). In the current study, AMAT provides the functionality to model curved flight paths associated with turning flight. For the turning flight cases examined here, the flight path in AMAT is defined using discrete waypoints on a semicircular trajectory (see Fig. 2). For this study, 21 waypoints were used to define the semicircular trajectory. The 19x19 hemisphere used at each of these waypoints is the same (because all cases are steady state), but oriented at each waypoint such that the front of the hemisphere always points in the direction of flight. For a straight flight path cases examined here, the flight path was defined using two waypoints (start and end points) in AMAT. In all cases, the “top” of the hemisphere is parallel to the flat ground. The vehicle can be banked, pitched, etc. inside the hemisphere. However, the vehicle orientation inside the hemisphere is accounted for by AARON and the vehicle is at the center of the hemisphere.

QUADROTOR MODELING

Figure 1a shows the rotor rotation direction and rotor numbering scheme. The right-front and left-rear rotors (rotors 1 and 4, respectively) turn counterclockwise, and the left-

front and right-rear rotors (rotors 2 and 3, respectively) turn clockwise. The CAMRAD II model of the quadrotor is summarized as follows (Refs. 2 and 4): four rotors, rigid uniform blades, collective control, constant RPM, rolled-up free wake (single tip vortex), and longitudinal trim (net zero average vertical and horizontal forces and pitching moment about the aircraft center of gravity). The blades have uniform spanwise inertial and stiffness properties; the blade root includes flap hinge and a pitch bearing. Aerodynamically, the rotors are coupled using wake induced velocities from all rotors. This setting is likely to be the most accurate depiction of the phenomena, capturing potentially important interactions due to strong vortices from not only the other blades on the same rotor, but also from blades of another rotor (rotor-rotor interaction). AARON calculates the 1/3-octave band spectrum at each point of a 19x19 hemisphere (with a radius of 27R and with 10 degree spacing in both the fore/aft and the lateral directions) underneath the vehicle. The noise calculation is based on the CAMRAD II outputs and a small amount of supplemental information and includes both tonal sources (thickness and loading noise) and broadband noise (trailing edge self noise), see Ref. 1. AMAT is used to model curved flight paths associated with turning flight.

RESULTS

Noise predictions for three steady maneuvers (level, descending, and climbing turns, shown in Fig. 2) are obtained for the 550/3 concept vehicle (tip speed is 550 ft/sec, with three blades per rotor). The rotor blade radius is 9 ft, and the RPM is 577. The flight speed is 122 kts. Descent and climb are performed at a 6 deg inclination. The banked turn rate in both directions is 3 deg/sec, resulting in a bank (roll) angle of approximately 19 deg. Results are presented for three microphone locations: a microphone on the centerline of the flight track, a microphone 150 m (492 ft) to the left of the center microphone, and a microphone 150 m to the right of the center microphone. The three microphones are located 4 ft above the ground.

Results are presented separately for each maneuver condition and include the following:

- Quadrotor trim and performance quantities
- Contour plots (front right rotor, # 1) for the vertical blade loading (“loadz”) and its derivative. loadz is in the airframe frame
- Azimuthal loadz and its derivative at 0.765R
- Quadrotor noise predictions (OASPLmax and EPNL).

Level turns

Quadrotor trim and performance, level turns. Results for level straight flight and level turns are shown in Figs. 3a-3i. The trim and performance quantities shown include the blade collective, quadrotor pitch and roll, rotor thrust and power. Figures 3a-3b show the average collective and quadrotor pitch and roll angles required for trim. Figure 3f shows that the

interference power is very small (with small increases in the rear rotors, # 3 and 4); Fig. 3e shows the same effect for the total power. Propulsive power (Fig. 3i) is the largest contributor to the total power, with roughly equal contributions from the induced and profile components (Figs. 3g-3h).

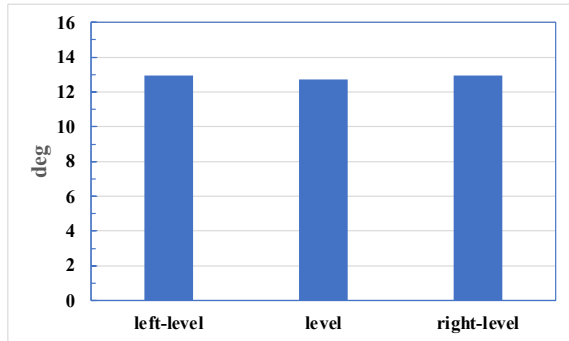


Figure 3a. Collective, average, level flight and level turns.

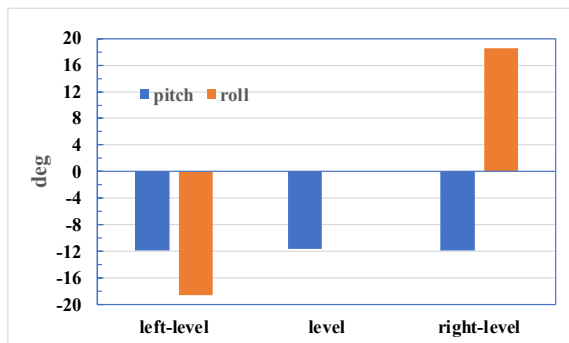


Figure 3b. Quadrotor pitch and roll, level flight and level turns.

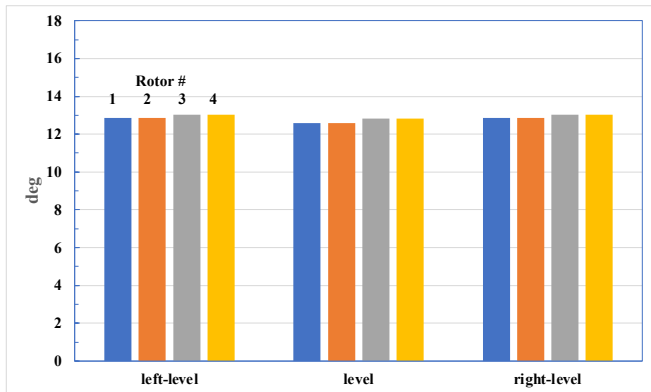


Figure 3c. Collective, rotors 1-4, level flight and level turns.

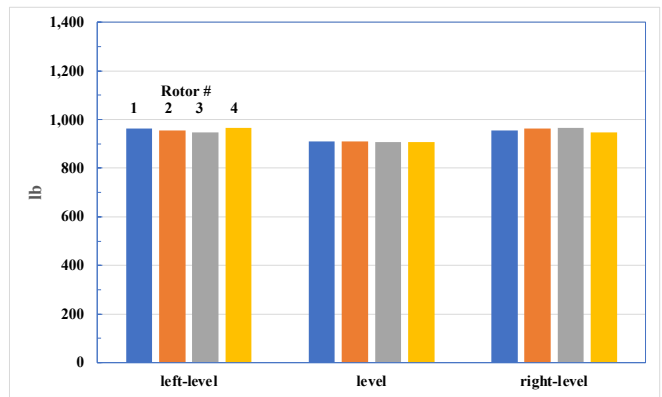


Figure 3d. Thrust, rotors 1-4, level flight and level turns.

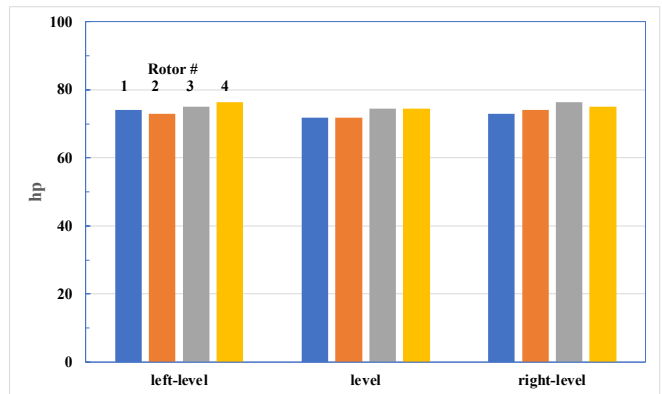


Figure 3e. Total power, level flight and level turns.

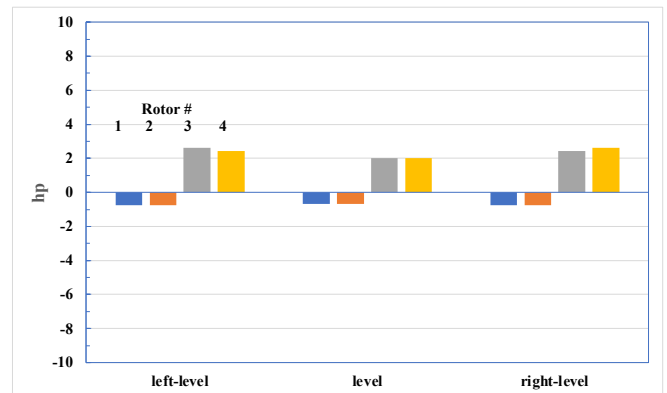


Figure 3f. Interference power, level flight and level turns.

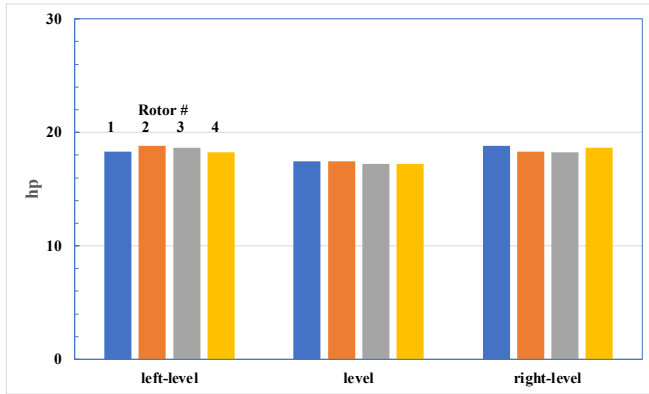


Figure 3g. Induced power, level flight and level turns.

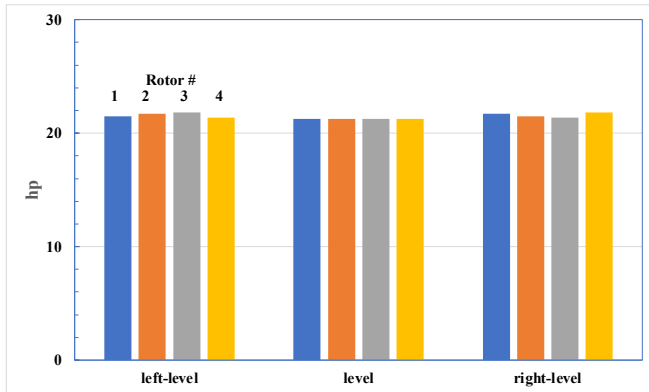


Figure 3h. Profile power, level flight and level turns.

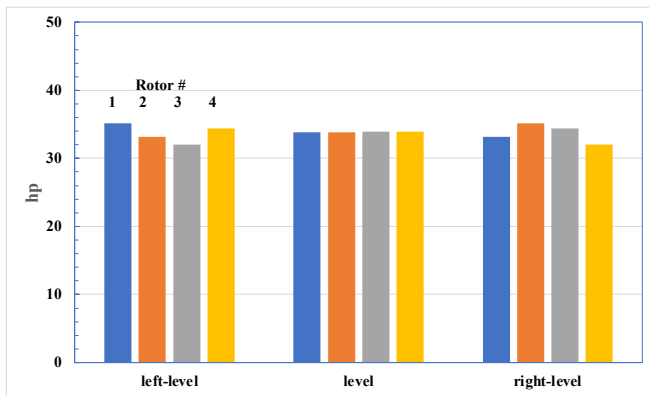


Figure 3i. Propulsive power, level flight and level turns.

Derivative of vertical blade loading, level turns. Results for only the front right rotor (# 1) are shown here because, for the 122 knots flyover considered in this study, rotor-rotor interference is small (Fig. 3f) compared to the 50 knots approach condition considered in Refs. 2 and 4 where the rear rotors are significantly influenced by the front rotors. Also, the front two rotors behave similarly and basic trends can be obtained from a study of only the front right rotor. Figures 4a-4d show vertical blade loading contours and 0.765R (represented by the dashed-line circle in Figs. 4a-4c) azimuthal variations for level flight and level turns. Figures

5a-5d show the corresponding loadz derivatives. The loadz derivatives are important because they are a leading contributor to the loading noise. The increased loading during turns is shown in Figs. 4a-4d, see the region near the front of the rotor. The contours for the left and right turns are largely similar (Figs.4b-4c), with slight variations between them (this can also be seen from Fig. 4d). Figures 4a-4d also show there is no significant BVI activity in level turns; the only “hot” spots are around 0 deg and 180 deg azimuths, i.e., the typical 2 per rev behavior in forward flight, seen clearly in Fig. 4d. Some BVI activity is seen in the 45-90 deg range which can be identified via loading spikes. The spikes in the azimuthal derivatives of loadz shown in Fig. 5d are consistent with the above observations, showing corresponding spikes. Figure 5d is similar in shape to a typical BVI time history that is seen in rotorcraft noise literature (for example, Fig. 6 of Ref. 15).

Quadrotor noise, level turns. Figure 6a shows the total, thickness plus loading (T+L), and broadband (BB) noise contributions to OASPLmax in level turns for the center microphone. The thickness noise is not a significant source (< 41 dBA) and is shown together with the loading noise (T+L). Broadband noise is 65 dBA and is the secondary source, with T+L noise being the primary source. Figure 6b shows the total OASPLmax in level turns for all three microphones. The center microphone noise level is the same in both turn directions and the turn noise level is lower than the level flight noise level (70 dBA compared to 76 dBA). A left turn increases the left side noise level compared to the right side; a right turn increases the right side noise level compared to the left side. Figure 6c shows EPNL and average EPNL for all three microphones, and the trends are the same as for OASPLmax. The center microphone EPNLavg is higher than that for the side microphones (81 vs. 78 EPNdB).

The results show that level straight flight has either higher or roughly the same noise levels compared to level turning flight on the side of the turn direction. To elaborate, the OASPLmax results of Fig. 6b show that for the:

- center microphone: noise levels are 76 and 70 dBA for level flight and level turning flight, respectively.
- side microphones: noise levels are roughly the same on the side of the turn direction for level turning flight (68 dBA) compared to level flight (69 dBA).

The OASPLmax results of Fig. 6b are consistent with the EPNL results of Fig. 6c. Thus, a UAM quadrotor in level straight flight has higher noise levels than in level turning flight. This is contrary to the Fly Neighborly guidelines (Ref. 9) on level flight that were developed for conventional single main rotor/tail rotor configurations “*Straight flight is quieter than turning flight.*”

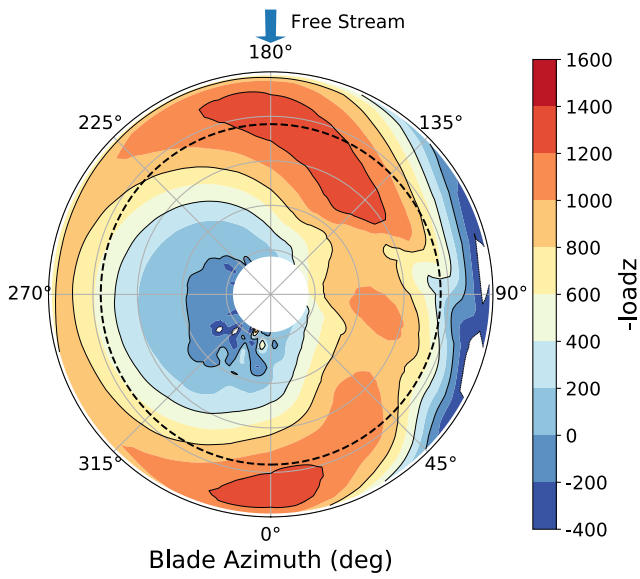


Figure 4a. loadz, level flight.

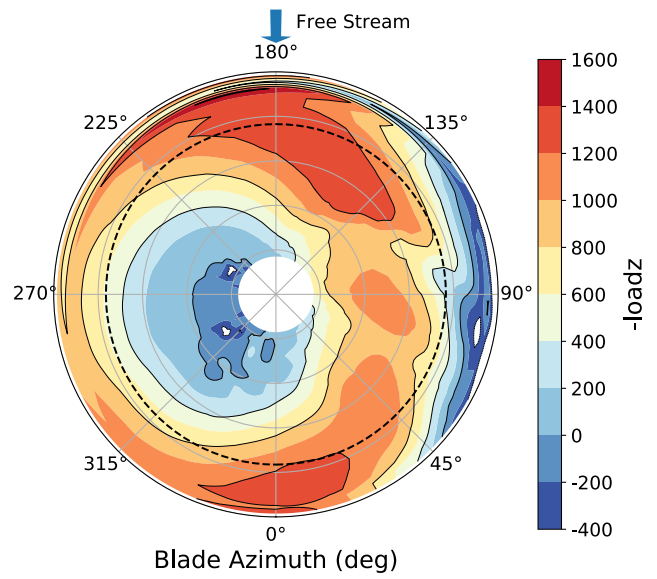


Figure 4c. loadz, level right turn.

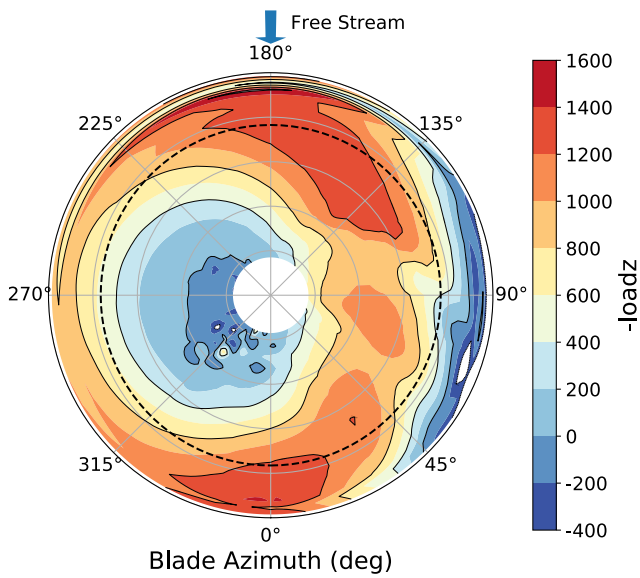


Figure 4b. loadz, level left turn.

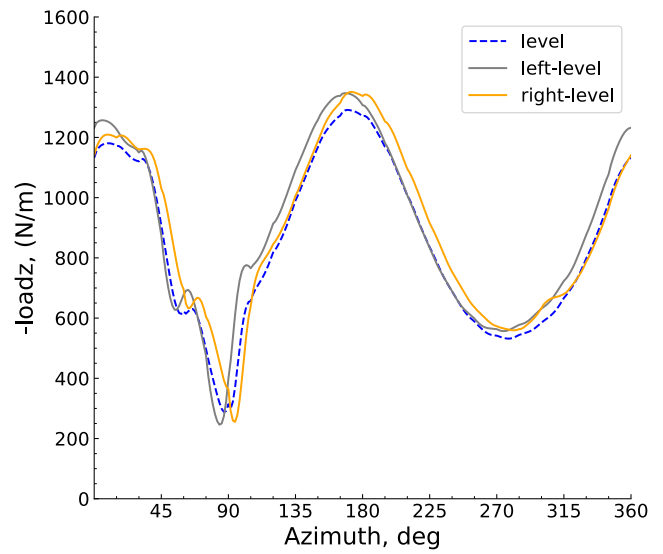


Figure 4d. 0.765R (dashed-line circle, Figs. 4a-4c)
loadz, level turns.

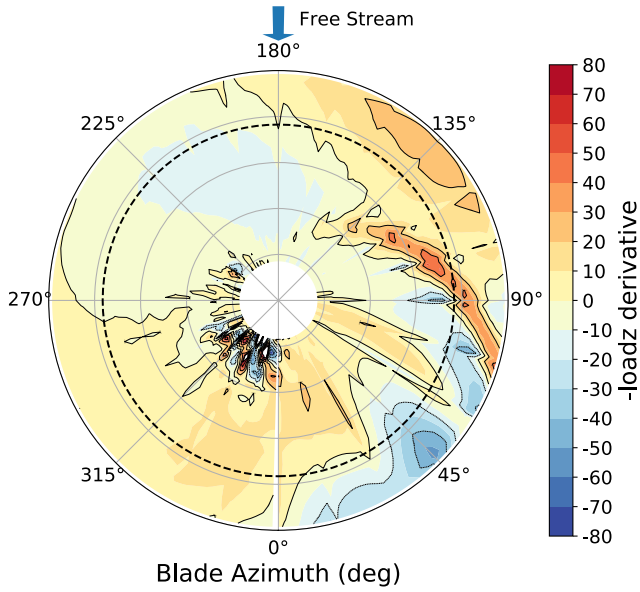


Figure 5a. loadz derivative, level flight.

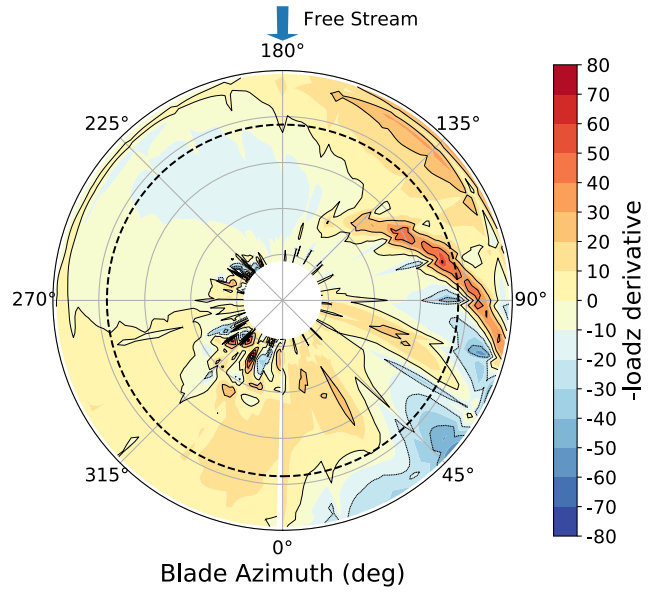


Figure 5c. loadz derivative, level right turn.

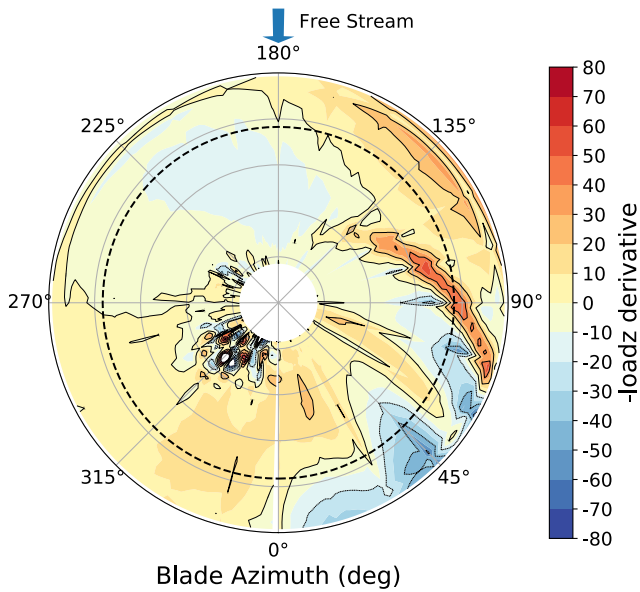


Figure 5b. loadz derivative, level left turn.

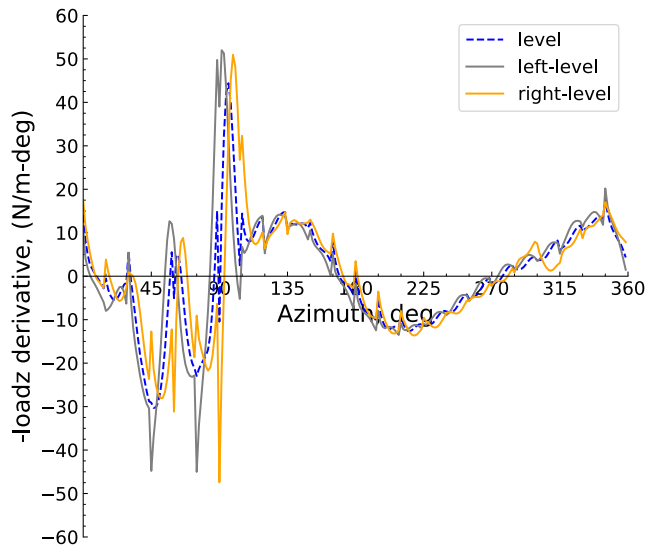


Figure 5d. 0.765R (dashed-line circle, Figs. 5a-5c)
loadz derivative, level flight and level turns

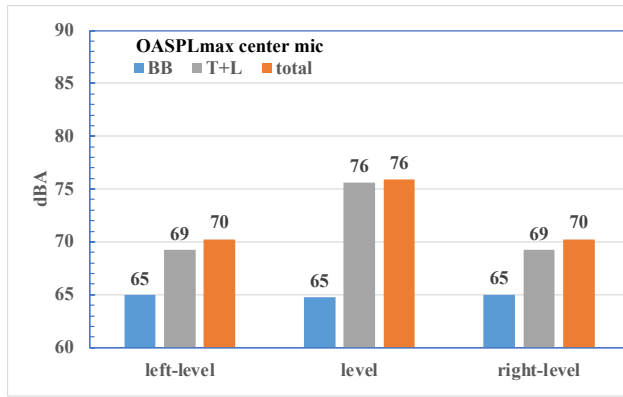


Figure 6a. Level flight and level turns OASPLmax (total, T+L, and BB), center microphone.

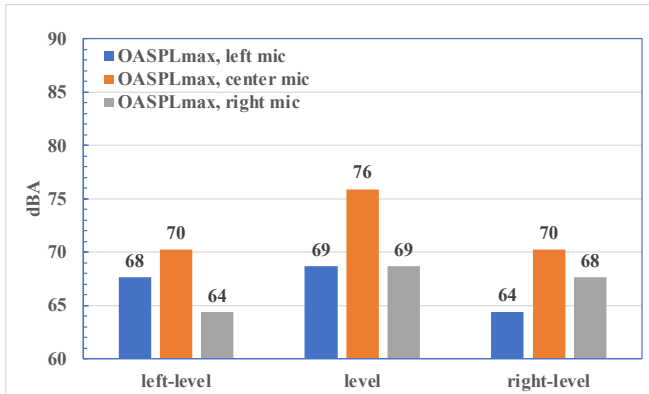


Figure 6b. Level flight and level turns total OASPLmax, three microphones.

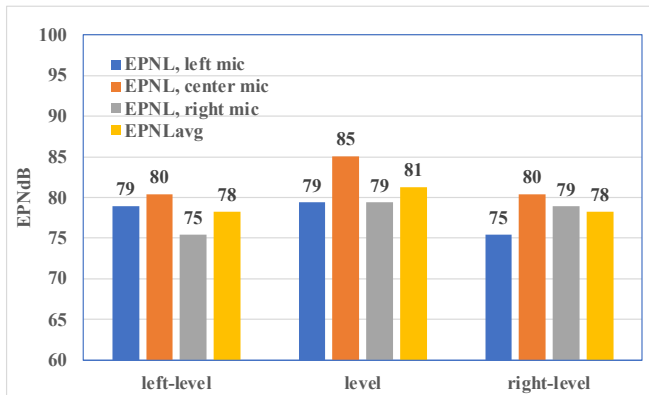


Figure 6c. Level flight and level turns EPNL, three microphones and average.

Descending turns

Quadrotor trim and performance, descending turns. Results for descending turns are shown in Figs. 7a-7i. The trim and performance quantities shown include the blade collective, quadrotor pitch and roll, rotor thrust and power. Figures 7a-7b show the average collective and quadrotor pitch and roll angles required for trim. Figure 7f shows that the interference

power is small relative to the total power (Fig. 7e), with increased power required for the rear rotors, # 3 and 4. The induced and profile powers are roughly the same magnitude (Figs. 7g-7h) and contribute equally to the total power.

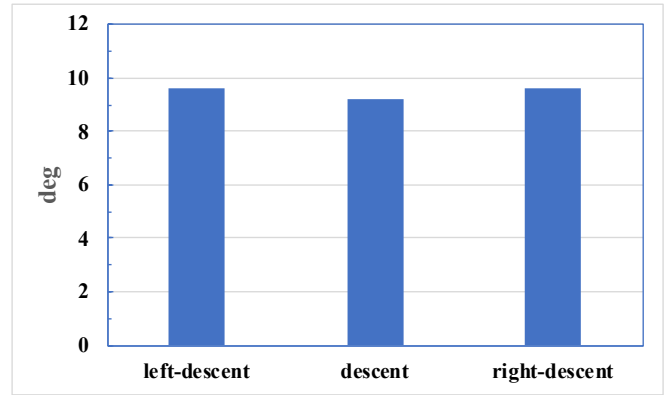


Figure 7a. Collective, average, descending flight and descending turns.

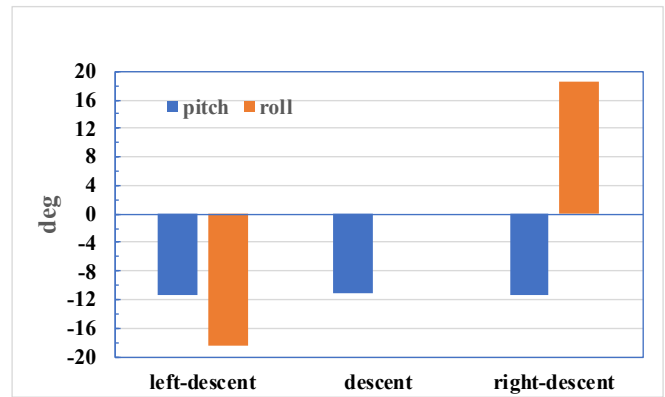


Figure 7b. Quadrotor pitch and roll, descending flight and descending turns.

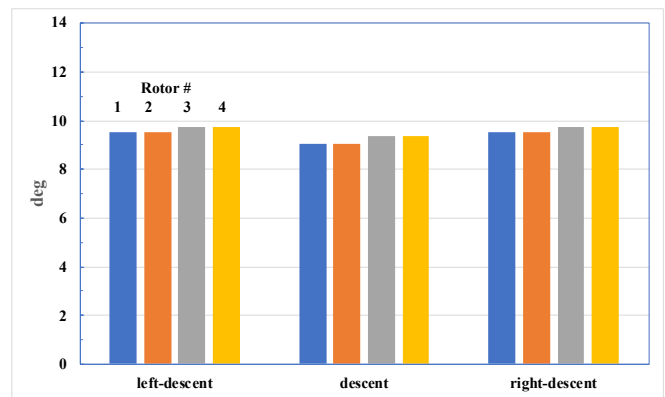


Figure 7c. Collective, rotors 1-4, descending flight and descending turns.

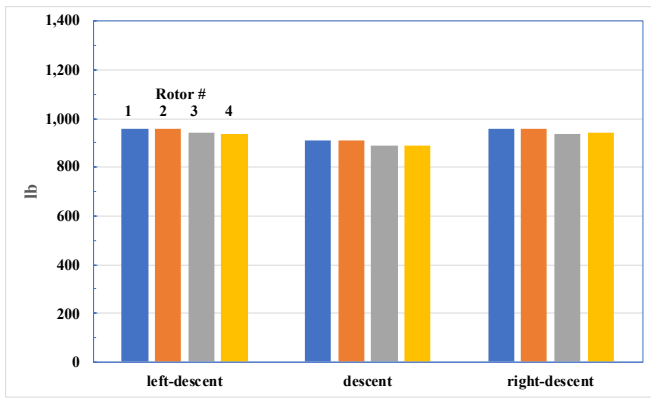


Figure 7d. Thrust, rotors 1-4, descending flight and descending turns.

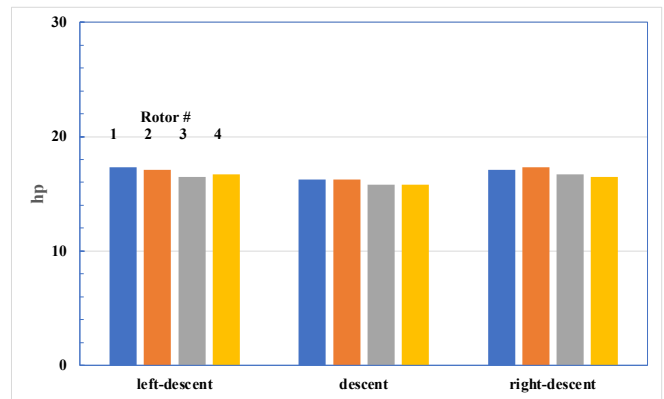


Figure 7g. Induced power, descending flight and descending turns.

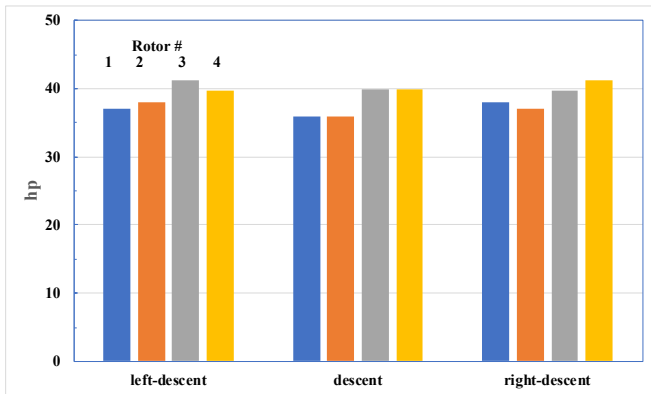


Figure 7e. Total power, descending flight and descending turns.

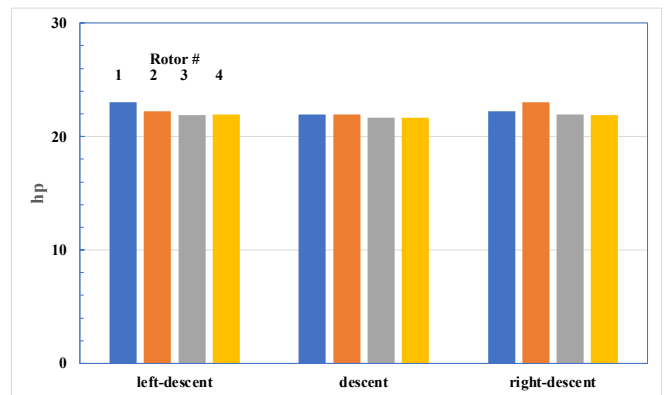


Figure 7h. Profile power, descending flight and descending turns.

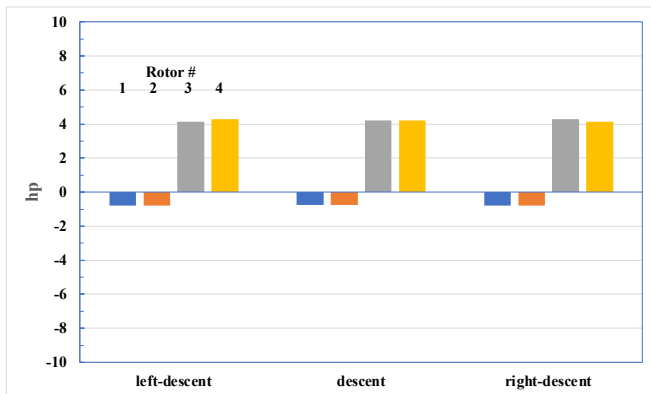


Figure 7f. Interference power, descending flight and descending turns.

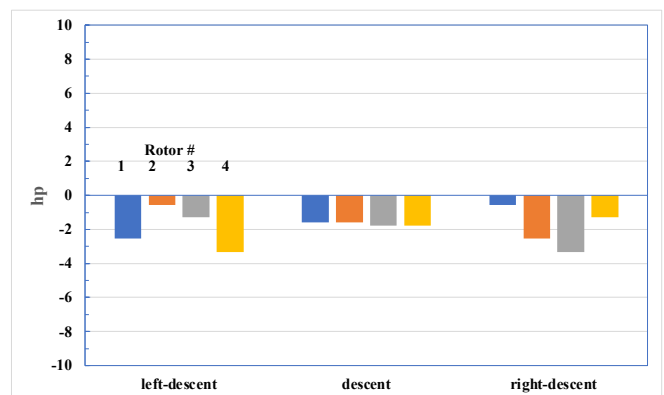


Figure 7i. Propulsive and climb power, descending flight and descending turns.

Derivative of vertical blade loading, descending turns. Results for only the front right rotor (# 1) are shown, as discussed in the section on level turns. Figures 8a-8d show vertical blade loading loadz contours and 0.765R azimuthal variations for straight line descent and descending turns. Figures 9a-9d show the corresponding loadz derivatives. The increased loading during turns can be seen in Figs. 8a-8d. The contours for the left and right turns are largely similar

(Figs.8b-8c), with slight variations between them (this can also be seen from Fig. 8d). Figures 8a-8d also show considerable BVI activity in descent and descending turns; several hot spots are present between 0 and 180 deg azimuths. At 0.765R, there is considerable BVI activity in the 0-135 deg range which shows loading spikes (Fig. 8d).

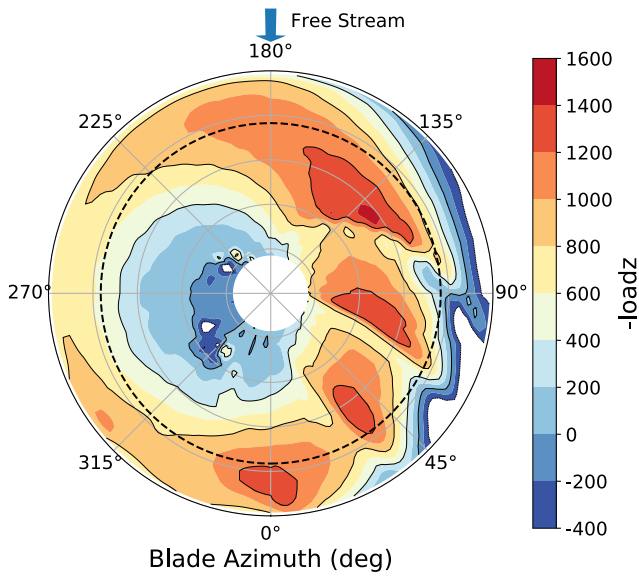


Figure 8a. loadz, descent.

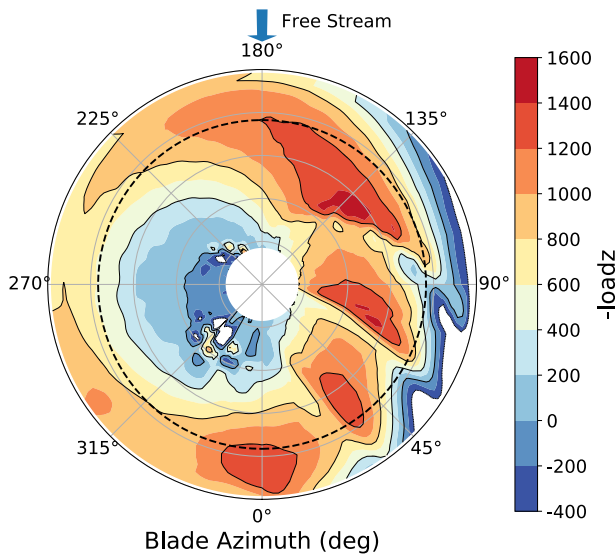


Figure 8b. loadz, descending left turn.

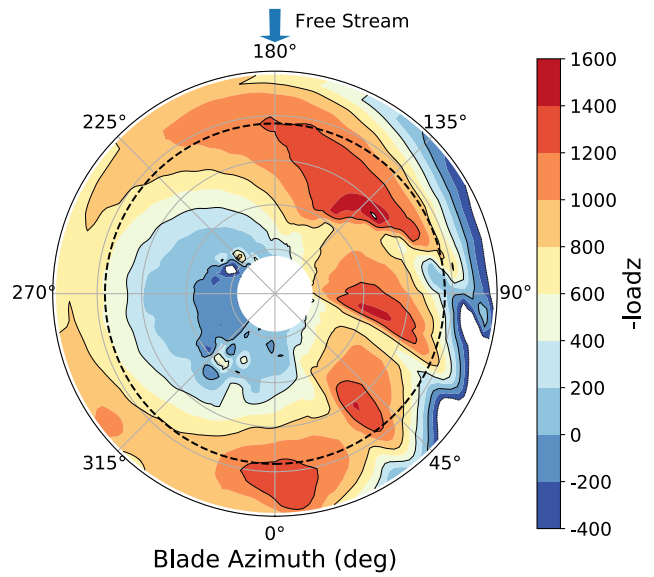


Figure 8c. loadz, descending right turn.

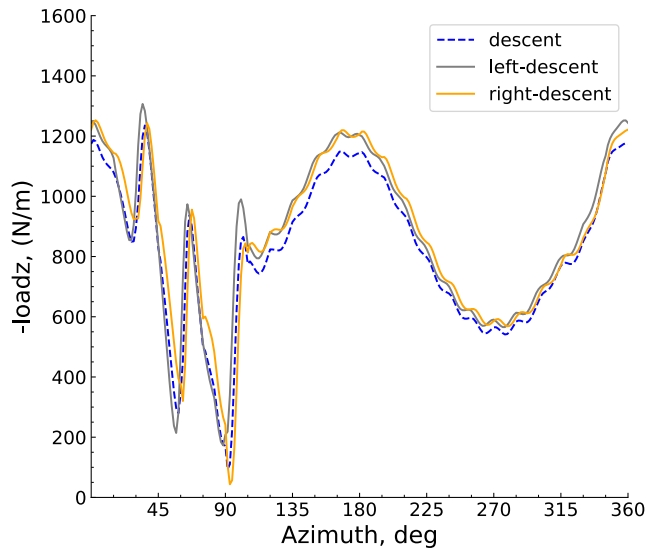


Figure 8d. 0.765R (dashed-line circle, Figs. 8a-8c) loadz, descending flight and descending turns.

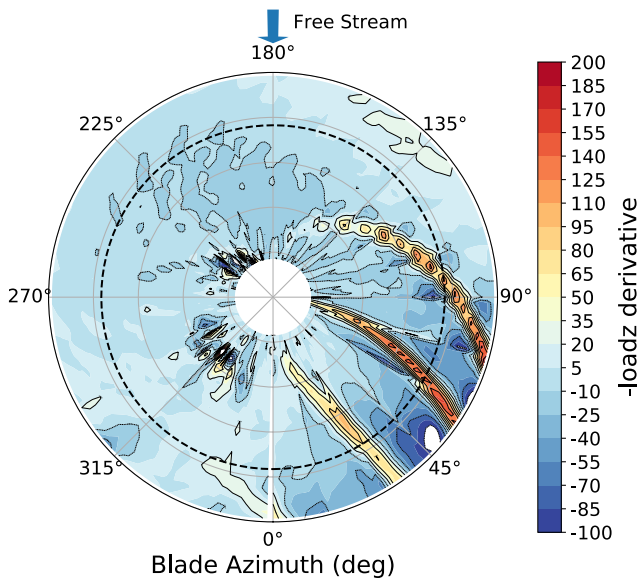


Figure 9a. loadz derivative, descent.

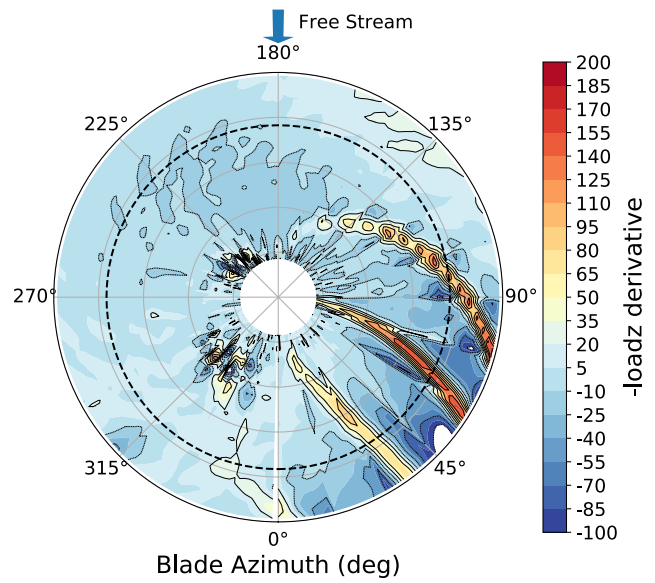


Figure 9c. loadz derivative, descending right turn.

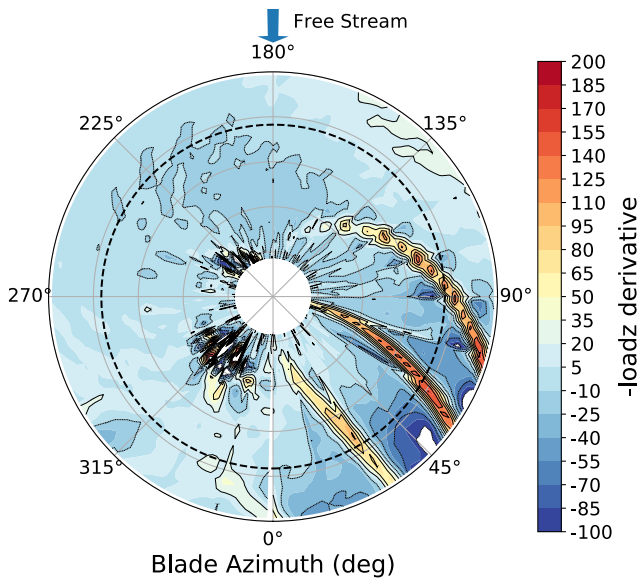


Figure 9b. loadz derivative, descending left turn.

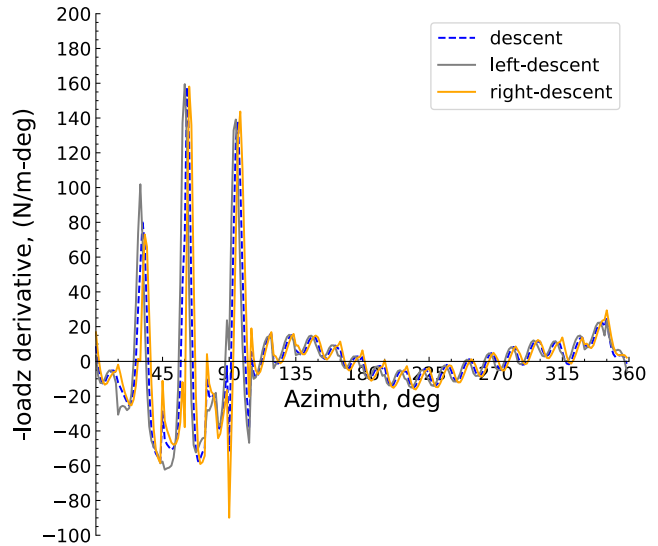


Figure 9d. 0.765R (dashed-line circle, Figs. 9a-9c) loadz derivative, descending flight and descending turns.

Quadrotor noise, descending turns. Figure 10a shows the total, T+L, and BB noise contributions to OASPLmax in straight descent and descending turns for the center microphone. The thickness noise is not significant (< 40 dBA) and is shown together with the loading noise (T+L). Broadband noise is around 65 dBA and is the secondary source, with T+L noise being the primary source. Figure 10b shows the total OASPLmax in descending turns for all three microphones. The center microphone noise level is the same in both turn directions and the turning noise level is lower than the level flight noise level (84 dBA compared to 80 dBA). Similar to the level flight condition, the descent noise level in the direction of the turn is larger compared to the opposite direction. Figure 10c shows EPNL and average EPNL for all

three microphones, and the trends are the same as for OASPLmax. The center and side microphones have roughly the same EPNLavg (within 1 dBA).

The results show that descending straight flight has either higher or roughly the same noise levels compared to descending turning flight on the side of the turn direction. To elaborate, the OASPLmax results of Fig. 10b show that for the:

- a) center microphone: noise levels are 84 and 80 dBA for straight descent and descending turning flight, respectively.
- b) side microphones: noise levels are roughly the same on the side of the turn direction for descending turning flight (77 dBA) compared to straight descent (76 dBA).

The OASPLmax results of Fig. 10b are consistent with the EPNL results of Fig. 10c. Thus, a UAM quadrotor in descending straight flight has higher noise metrics than in descending turning flight.

A comparison of the noise in level and descending turns (Figs 6b, 6c vs. 10b, 10c, respectively) shows that level turns have lower noise levels than descending turns. This current conclusion for UAM quadrotors is consistent with the Fly Neighborly guidelines developed for conventional single main rotor/tail rotor helicopter configurations (Ref. 9) for descending flight “*Level turns are quieter than descending turns.*”

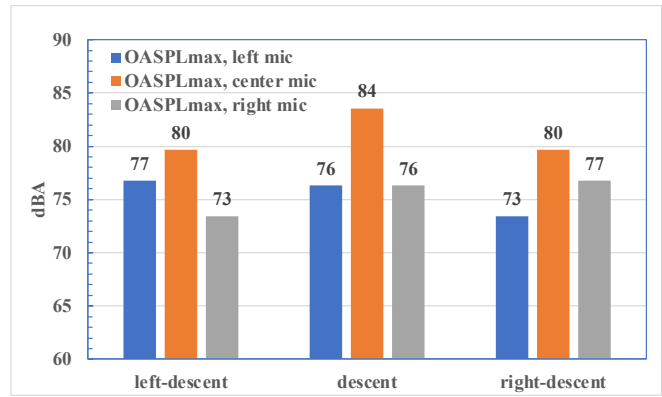


Figure 10b. Descent and descending turns total OASPLmax, three microphones.

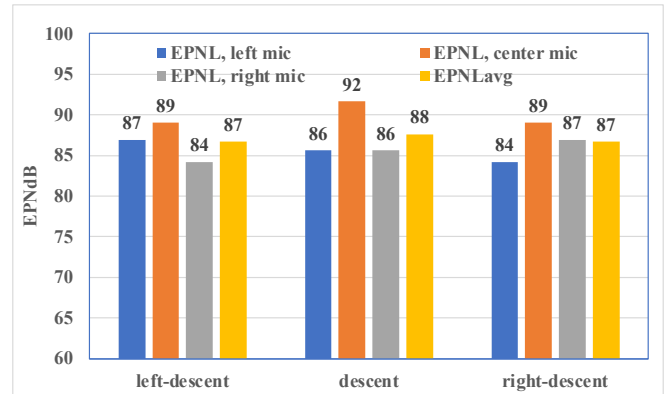


Figure 10c. Descent and descending turns EPNL, three microphones and average.

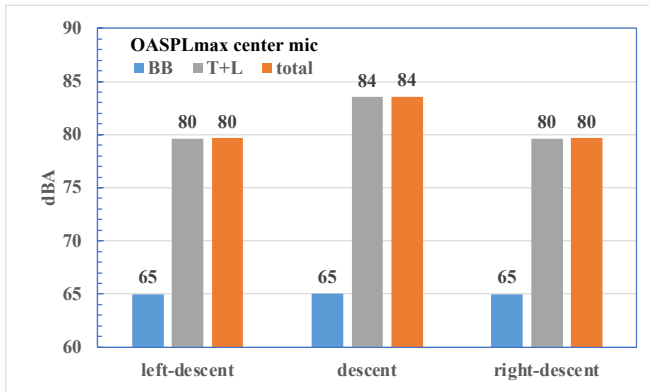


Figure 10a. Descent and descending turns OASPLmax (total, T+L, and BB), center microphone.

Climbing turns

Quadrotor trim and performance, climbing turns. Results for straight climb and climbing turns are shown in Figs. 11a-11i. Figure 11f shows that the interference power in climbing turns is very small, with the induced and profile powers roughly equal (Figs. 11g-11h). As expected, the propulsive and climb power (Fig. 11i) is the largest contributor to total power in this flight condition.

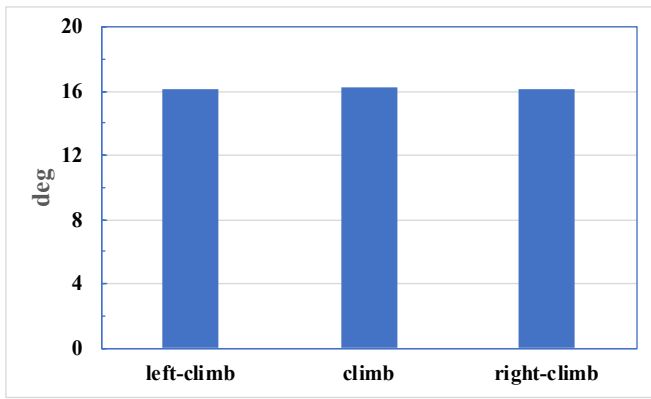


Figure 11a. Collective, average, climb and climbing turns.

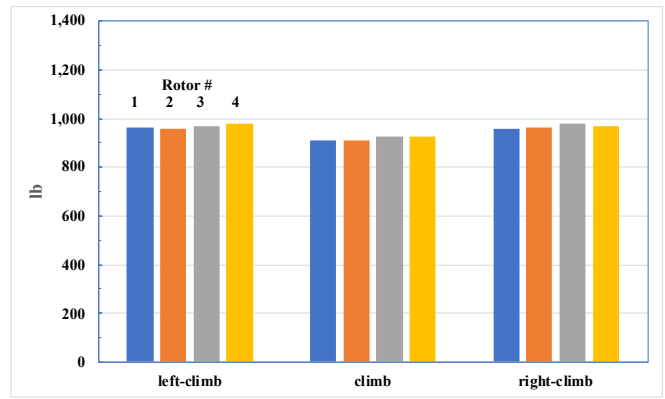


Figure 11d. Thrust, rotors 1-4, climb and climbing turns.

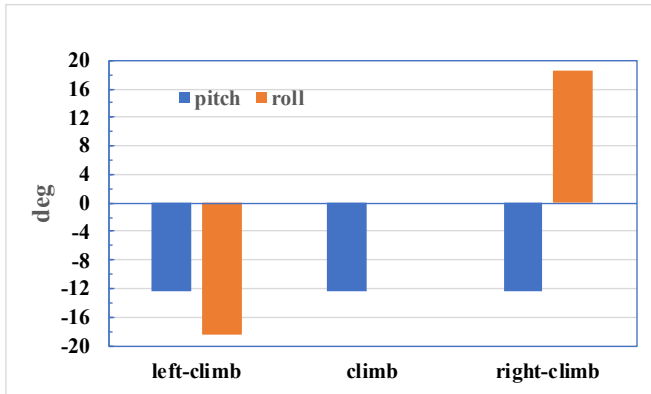


Figure 11b. Quadrotor pitch and roll, climb and climbing turns.

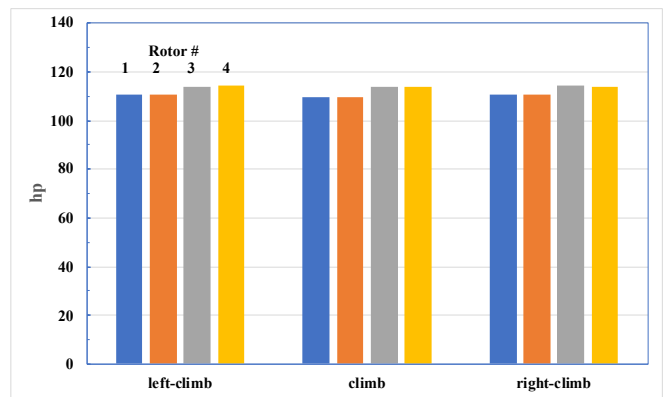


Figure 11e. Total power, climb and climbing turns.

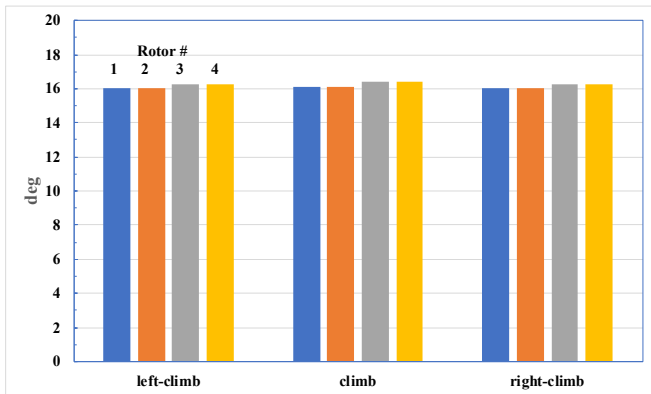


Figure 11c. Collective, rotors 1-4, climb and climbing turns.

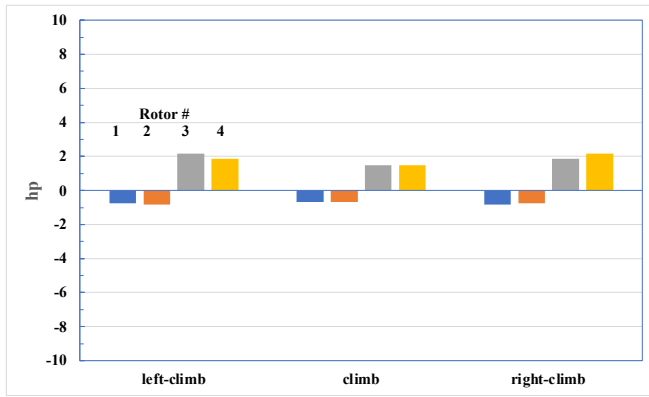


Figure 11f. Interference power, climb and climbing turns.

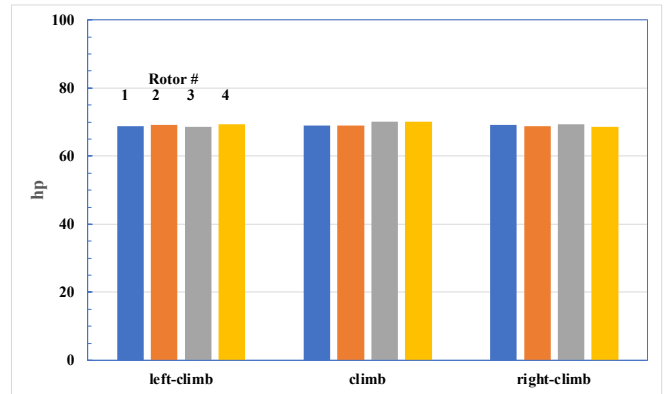


Figure 11i. Propulsive and climb power, climb and climbing turns.

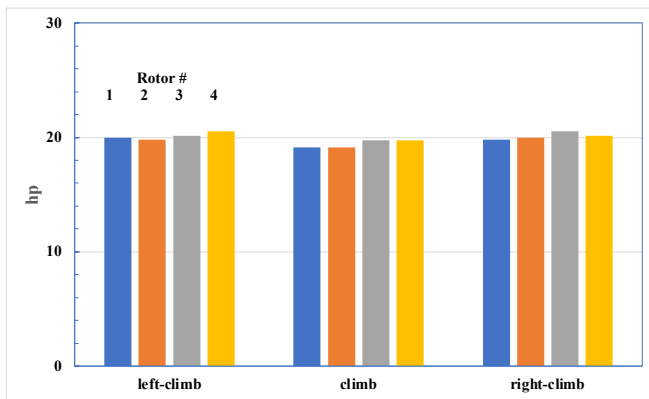


Figure 11g. Induced power, climb and climbing turns.

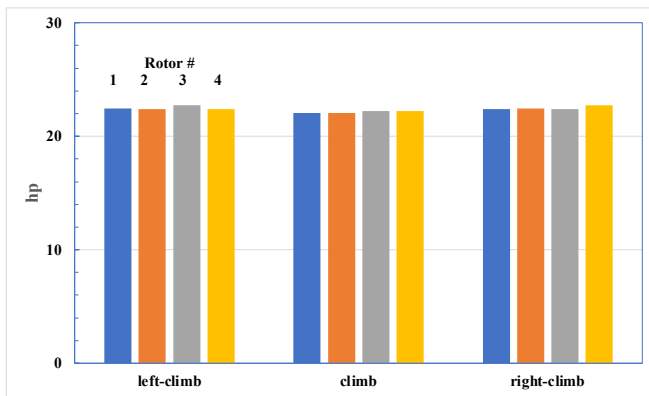


Figure 11h. Profile power, climb and climbing turns.

Derivative of vertical blade loading, climbing turns. Results for only the front right rotor (# 1) are shown, as has been discussed in previous sections. Figures 12a-12d show vertical blade loading loadz contours and 0.765R azimuthal variations for straight climb and climbing turns. Figures 13a-13d show the corresponding loadz derivatives. The increased loading during turns can be seen in Figs. 12a-12d which show loadz. The contours for the left and right turns are largely similar (Figs.12b-12c), with slight variations between them (this can also be seen from Fig. 12d). Figures 12a-12d also show there is no BVI activity in climbing turns; the only “hot” spots are around 0 deg and 180 deg azimuths, i.e., the typical 2 per rev behavior in forward flight, seen clearly in Fig. 12d.

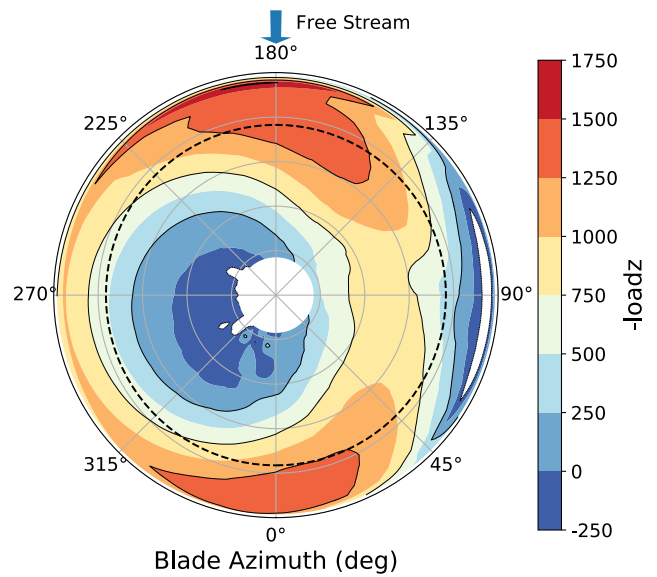


Figure 12a. loadz, climb.

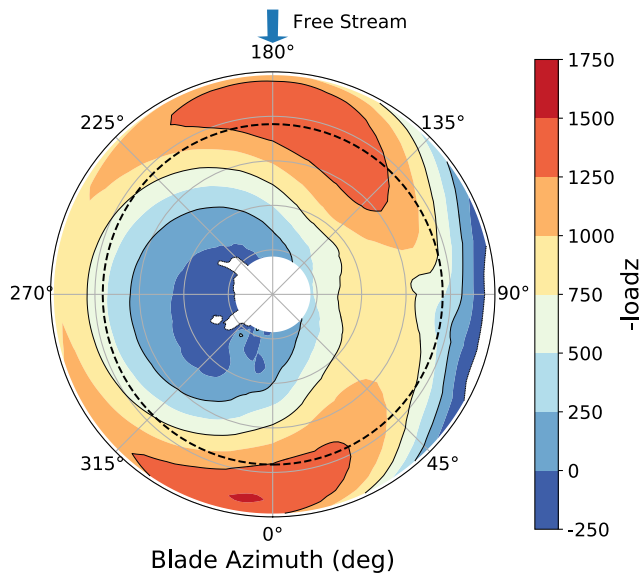


Figure 12b. loadz climbing left turn.

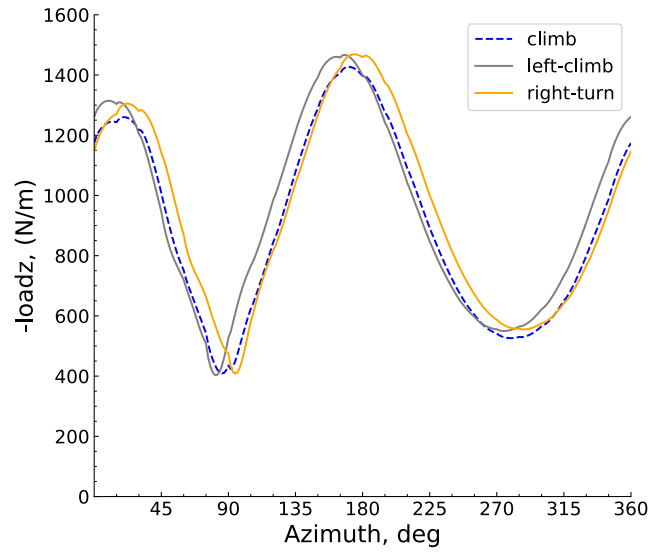


Figure 12d. 0.765R(dashed-line circle, Figs. 12a-12c) loadz, climbing turns.

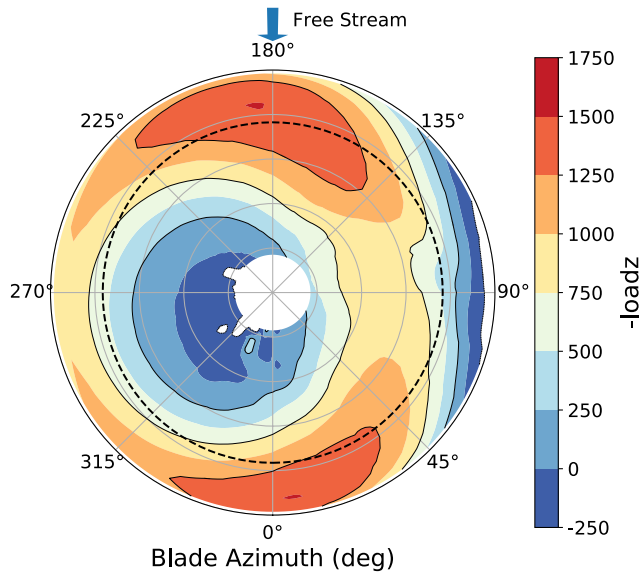


Figure 12c. loadz climbing right turn.

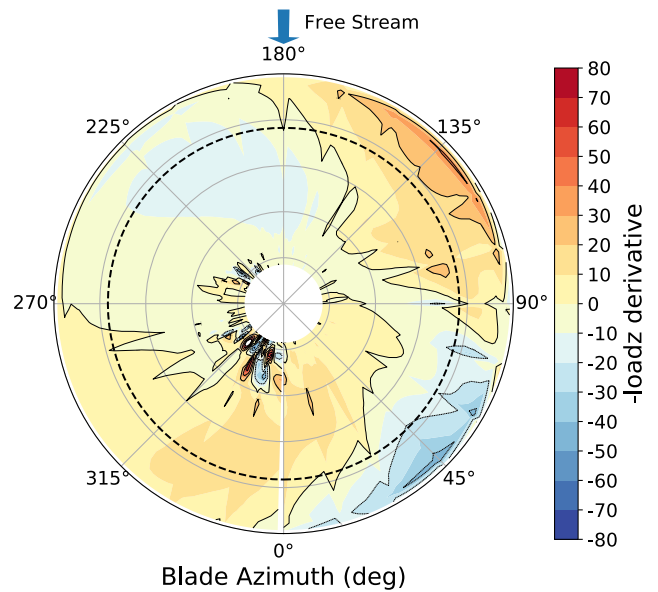


Figure 13a. loadz derivative climb.

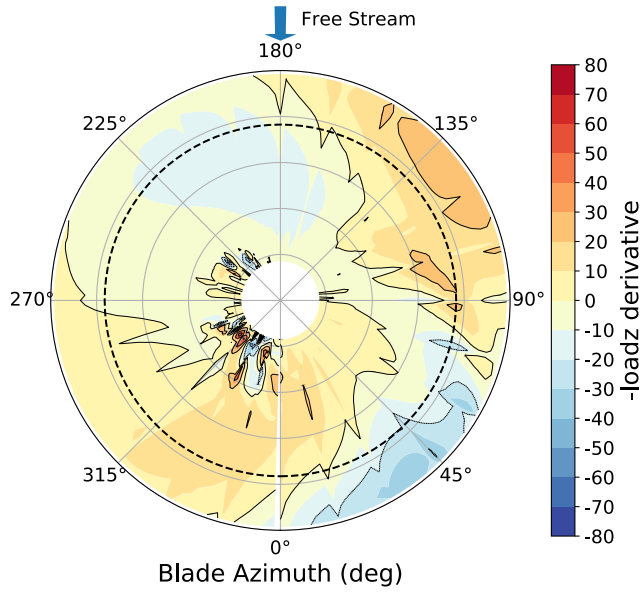


Figure 13b. loadz derivative climbing left turn.

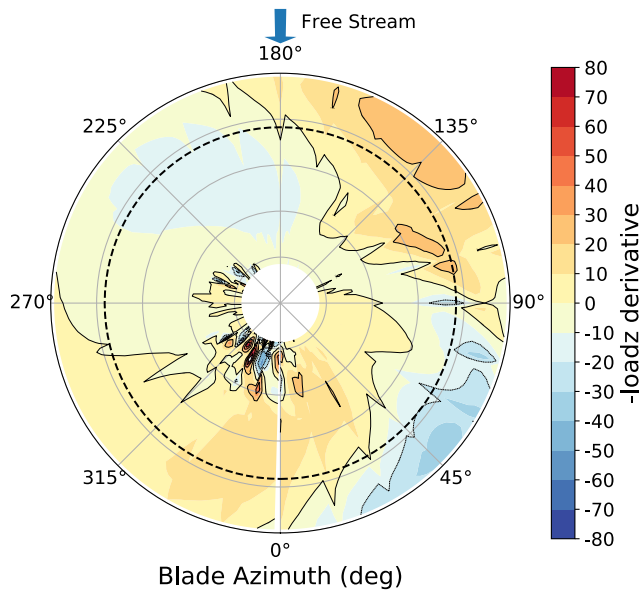


Figure 13c. loadz derivative climbing right turn.

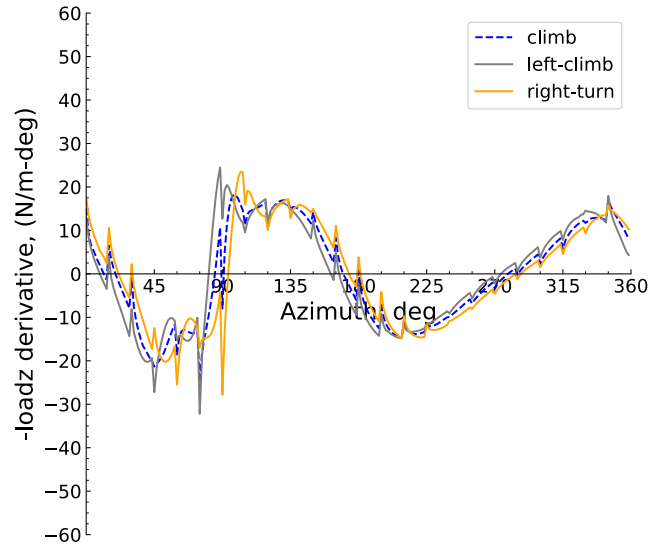


Figure 13d. 0.765R (dashed-line circle, Figs. 13a-13c) loadz derivative, climb and climbing turns.

Quadrotor noise, climbing turns. Figure 14a shows the total, T+L, and BB noise contributions to OASPLmax in climbing turns for the center microphone. The thickness noise is not important (< 43 dBA) and is shown together with the loading noise (T+L). Broadband noise is 65 dBA and close to T+L noise level, with T+L noise still being the primary source. Figure 14b shows the total OASPLmax in climbing turns for all three microphones. The center microphone noise level is the same in both turn directions and the turning noise level is lower than the straight climb flight noise level (68 dBA compared to 72 dBA). Similar to level and descending flight conditions, the climb noise level in the direction of the turn is larger compared to the opposite direction. Figure 6c shows EPNL and average EPNL for all three microphones. Climbing turns affect only the center microphone EPNL (79 EPNdB in climbing turns and 81 EPNdB in straight climb). The noise levels for the side microphones are not sensitive to the turn direction (76-77 EPNdB).

The results show that climbing straight flight has either higher or roughly the same noise levels compared to climbing turning flight on the side of the turn direction. To elaborate, the OASPLmax results of Fig. 14b show that for the:

- a) center microphone: noise levels are 72 and 68 dBA for straight climb and climbing turning flight, respectively.
- b) side microphones: noise levels are roughly the same on the side of the turn direction (65 dBA) for straight climb and climbing turning flight.

The OASPLmax results of Fig. 14b are consistent with the EPNL results of Fig. 14c. Thus, a UAM quadrotor in climbing straight flight has higher noise metrics than in climbing turning flight. A Fly Neighborly guideline for climbing flight

may not exist and so no comparison is possible with the guideline.

Finally, compared to level and descending turns, climbing turns are the quietest (Figs. 6b, 10b, and 14b.)

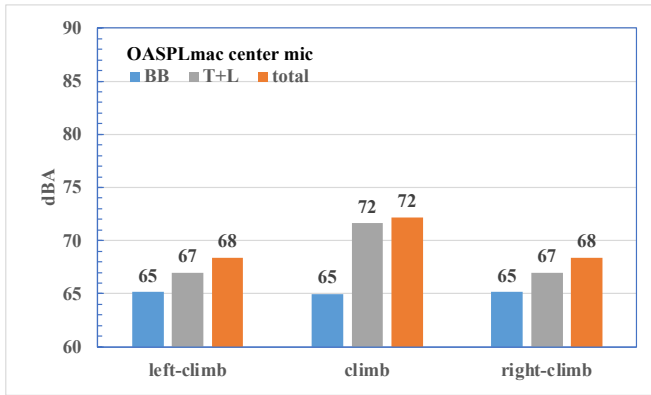


Figure 14a. Climb and climbing turns OASPLmax (total, T+L, and BB), center microphone.

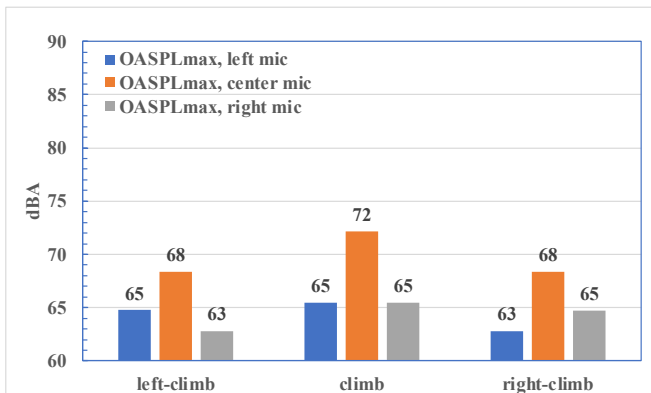


Figure 14b. Climb and climbing turns total OASPLmax, three microphones.

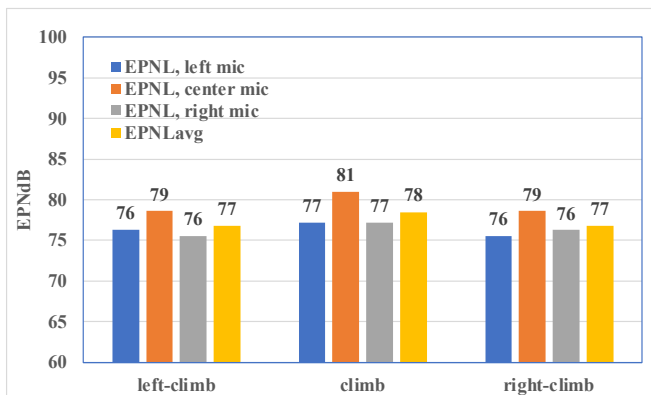


Figure 14c. Climb and climbing turns EPNL, three microphones and average.

CONCLUSIONS

This study examined whether the HAI Fly Neighborly operational recommendations that are based on single main rotor/tail rotor configurations hold for an example of a UAM-class vehicle with multiple rotors. Predictions were made for three steady maneuvers: level turns, descending turns, and climbing turns. The 6-occupant quadrotor concept vehicle designed under the NASA Revolutionary Vertical Lift Technology (RVLT) Project was considered. The tip speed is 550 ft/sec, with three blades per rotor (550/3). The RVLT Toolchain was exercised using CAMRAD II, pyaaron/AARON/ANOPP2 and a beta version of AMAT. AMAT provides functionality to acoustically model the curved flight paths associated with turning flight. Quadrotor trim and performance, contour plots of the vertical blade loading (loadz) and its derivative, and 0.765R azimuthal variations of loadz and its derivative were studied. Quadrotor noise trends in maneuvers were analyzed using maximum OASPL and EPNL.

Specific conclusions are as follows (noise related findings are based on predictions for the center microphone):

1. Trim and performance: Interference power for the flight conditions considered was relatively small compared to the total power. This result implies that for the current straight and turning flight conditions at 122 knots, the rotor-rotor interaction is not significant.
2. Vertical blade loading (loadz) and its derivative: As expected, loadz increased during turning flight. The azimuthal variations of the loadz derivative in level flight/level turns and descent/descending turns were similar in shape to typical BVI time histories.
3. BVI activity: Descending flight (straight and turns) involves the most BVI activity, followed by level flight (straight and turns), with climbing flight (straight and turns) having no BVI activity.
4. Straight descent and descending turns had the highest acoustic metrics. Straight climb and climbing turns had the lowest acoustic metrics, with straight level flight and level turns falling in between. In terms of the acoustic metrics examined: descent > level > climb. Here, the metrics were the A-weighted maximum OASPL and EPNL.
5. The Fly Neighborly guideline that addresses descents (“Level turns are quieter than descending turns”) holds for the UAM quadrotor as well. Descent generally involves increased BVI activity, and this conclusion may be reflecting this basic physical phenomenon common to all rotorcraft (with single or multiple main rotors).

6. Contrary to the Fly Neighborly guideline on level flight (“*Straight flight is quieter than turning flight*”), the UAM quadrotor in straight flight (whether level, descending, or climbing) has higher noise metrics than the corresponding turning flight condition. This finding may be related to the effect of multiple rotors and needs further study.
7. The Fly Neighborly guideline regarding the preferred turn direction (*turning away from the advancing blade is quieter than turning into the advancing blade*) does not hold for the quadrotor. As shown in Fig. 1a, the opposite rotation direction of the left and right rotors results in the same noise metrics whether turning left or right.

Author contact:

Sesi Kottapalli	sesi.b.kottapalli@nasa.gov
Christopher Silva	christopher.silva@nasa.gov
Doug Boyd	d.d.boyd@nasa.gov

ACKNOWLEDGMENTS

Insightful discussions with the following colleagues are gratefully acknowledged: Wayne Johnson, Gloria Yamauchi, Bill Warmbrodt, and Leonard Lopes.

REFERENCES

1. Silva, C. and Johnson, W., “Practical Conceptual Design of Quieter Urban VTOL Aircraft,” The Vertical Flight Society 77th Annual Forum Proceedings, Virtual, May 2021.
2. Kottapalli, S. and Silva, C., “Prediction of Quadrotor Acoustics Using RVL Toolchain,” VFS Aeromechanics for Advanced Vertical Flight Technical Meeting, San Jose, CA, January 2022.
3. Yamauchi, G., “A Summary of NASA Rotary Wing Research: Circa 2008–2018,” NASA/TP 2019-220459, December 2019.
4. Kottapalli, S., Silva, C., and Boyd, D. D., Jr. “Effect of Rotor Blade Elasticity on UAM Quadrotor Acoustics,” Vertical Flight Society 79th Annual Forum Proceedings, West Palm Beach, FL, May 2023.
5. Brentner, K. S. and Jones, H. E., “Noise Prediction for Maneuvering Rotorcraft,” Paper AIAA 2000–2031, 6th AIAA/CEAS Aeroacoustics Conference Proceedings, Lahaina, HI, June 2000.
6. Brentner, K. S., Perez, G., and Brès, G. A., “Toward a Better Understanding of Maneuvering Rotorcraft Noise,” Vertical Flight Society 58th Annual Forum Proceedings, Montreal, Canada, May 2002.
7. Greenwood, E., Schmitz, F. H., and Gopalan, G., “Helicopter External Noise Radiation in Turning Flight: Theory and Experiment,” Vertical Flight Society 71st Annual Forum Proceedings, Virginia Beach, VA, May 2015.
8. Stephenson, J. H., Watts, M. E., Greenwood, E., and Pascioni, K. A., “Development and Validation of Generic Maneuvering Flight Noise Abatement Guidance for Helicopters,” *Journal of the American Helicopter Society*, Vol. 67, 012012 (2022), DOI: 10.4050/JAHS.67.012012, 2022.
9. Helicopter Association International (HAI) Fly Neighborly guidelines: <https://rotor.org/wp-content/uploads/2021/07/Fly-Neighborly-Tips-Flyer-2019.pdf>
10. Johnson, W., “CAMRAD II, Comprehensive Analytical Model of Rotorcraft Aerodynamics and Dynamics,” Johnson Aeronautics, Palo Alto, CA, 1992-1999.
11. Meyn, L., “Rotorcraft Optimization Tools: Incorporating Rotorcraft Design Codes into Multi-Disciplinary Design, Analysis, and Optimization,” AHS Technical Meeting on Aeromechanics Design for Vertical Lift, San Francisco, CA, January 2018.
12. Lopes, L. V. and Burley, C. L., “ANOPP2 User’s Manual,” NASA/TM-2016-219342, October 2016.
13. Lopes, L. V., “ANOPP2 Mission Analysis Tool (AMAT),” UAM Noise Working Group (UNWG), Subgroup 1 Meeting, Hampton, VA, December 2022.
14. Rizzi, S. A., Letica, S. J., Boyd, D. D. Jr., and Lopes, L. V., “Prediction of Noise-Power-Distance Data for Urban Air Mobility Vehicles,” *Journal of Aircraft*, <https://doi.org/10.2514/1.C037435>, October 2023.
15. Yamauchi, G. K., Signor, D. B., Watts, M. E., Hernandez, F. J., and LeMasurier, P., “Flight Measurement of Blade-Vortex-Interaction Noise Including Comparison with Full-Scale Wind Tunnel Data,” American Helicopter Society 49th Annual Forum Proceedings, St. Louis, MO, May 1993. Also published as NASA-TM-112385, 1993.